FOREX Publication
Open Access | Rapid and quality publishing

International Journal of
Electrical and Electronics Research (IJEER)
Research Article | Volume 14, Issue 2 | Pages 424-435 | e-ISSN: 2347-470X

Drone Localization Estimation Using Wireless Sensor Network and Deep-Learning Techniques

Yaseen Naser Jurn[1*], Ekhlas Khalaf Gbashi[2], Abeer Tariq Maolood[3], and Sarah J. Mohammed[4]

[1]*Assist. Professor, College of Engineering, University of Information Technology and Communications, Baghdad, Iraq*
[2]*Professor, College of Computer Science, University of Technology, Baghdad, Iraq*
[3]*Professor, College of Computer Science, University of Technology, Baghdad, Iraq*
[4]*Lecturer, College of Computer Science, University of Technology, Baghdad, Iraq*

***Correspondence:** *yaseen.naser@uoitc.edu.iq*

ABSTRACT- This paper presents a powerful hybrid localization model of drones to be used in GPS-denied areas through the combination of Long Short-Term Memory (LSTM) networks with an Extended Kalman Filter (EKF). The system network is based on a Wireless Sensor Network (WSN) in which sensors are arranged in equilateral triangle triples to enable the combination of the Angle-of-Arrival (AoA) and Time-Difference-of-Arrival (TDoA) measurements. The traditional EKF only model may not be good with complex residual dynamics as well as motion uncertainties but the LSTM component is specifically used to model these nonlinearities which gives much better state estimation compared to what conventional kinematic models can offer.

The work presents a strict theoretical framework of triangular anchor geometry using Dilution of Precision (DOP) analysis and applying the nearest triple geometry to approximate localization using triangulation techniques when a drone goes into sensor field. Wide Monte Carlo simulation and statistical analysis with confidence intervals prove that the framework is very precise, that is, it can attain a distance error of less than 0.48 meters. Moreover, the suggested approach has shown a 42 percent reduction in Root Mean Square Error (RMSE) as compared to conventional EKF benchmarks. The contribution of each component is verified in detailed ablation studies, which prove that the system has the real-time computational performance required to deploy a drone in practice.

Keywords: Drone localization, UAV localization, WSN for drone localization, LSTM, AoA, DToA for drone localization, drone localization estimation, Kalman filter.

ARTICLE INFORMATION

Author (s): Yaseen Naser Jurn, Ekhlas Khalaf Gbashi, Abeer Tariq Maolood, and Sarah J. Mohammed;

Received: 24/08/25; **Accepted**: 03/05/26; **Published**: 25/06/26;
E- ISSN: 2347-470X;
Paper Id: IJEER 2408A16;
Citation: 10.37391/ijeer.140219
Webpage-link:
https://ijeer.forexjournal.co.in/archive/volume-14/ijeer-140219.html

Publisher's Note: FOREX Publication stays neutral with regard to jurisdictional claims in Published maps and institutional affiliations.

1. INTRODUCTION

Over the past ten years, unmanned aerial vehicles (UAVs) sometimes referred to as drones, have been increasingly popular in a variety of fields, including logistics, agriculture, cinematography, and surveillance systems. Furthermore, because of their combat capabilities—such as their small size, low altitude, and ability to fly at predefined coordinates—UAVs are employed to threaten several key areas. These features make it difficult to detect and track UAVs in real time [1]. Another significant use for drones is to provide wireless coverage [2-3]. Drones can be utilized in this deployment to support the current communication infrastructure by smoothly supplying wireless coverage in the service area. By enabling wireless connectivity between remote users without a direct communication link, it can also be utilized as a relay. This is can be considered as another type of risk of the UAVs on the important regions. Therefore, it is very dangerous at attack on the important regions. Hence, the early detection and localizing the UAV to prevent the potential risks.

In this paper, the primary goal is to use expert approaches to detect the drone localization at high accuracy. Each detecting unit in the suggested design is composed of three co-planar sensors that create an equilateral triangle, enabling accurate (AoA) and (TDoA) readings. The system uses deep learning to fuse input from many triplets to make the localization decision with great precision, achieving minimal error localization accuracy.

2. LITERATURE REVIEW

Numerous studies have suggested various methods for the two phases of UAV detection and localization based on various strategies in an effort to mitigate the risks associated with UAVs. In [4], an Extended Kalman Filter (EKF) based on Time Difference of Arrival (TDOA) measurements from a Wireless Sensor Network (WSN) was used to offer a real-time localization approach for (UAVs). Instead of using synchronized clocks, the system uses symmetric double-sided

FOREX Publication
Open Access | Rapid and quality publishing
International Journal of Electrical and Electronics Research (IJEER)
Research Article | Volume 14, Issue 2 | Pages 424-435 | e-ISSN: 2347-470X

two-way ranging (SDS-TWR) technology to measure the distances between the UAV and four base stations. In order to address security and safety concerns in sensitive areas, the work in [5] suggested two vision-based techniques for UAV localization employing dispersed ground sensors. The first technique, 2D-TPL, used elevation angles to determine altitude after estimating the UAV's horizontal projection using azimuth angles from several sensors. The second technique, 3D-TPL, was minimized distances to lines that are defined by angles measured by the sensor in order to directly estimate the UAV's 3D position. The work presented in [6], examines the relationship between antenna orientation and drone time-difference-of-arrival (TDOA) localization accuracy. Suggests a simplified model for antenna gain in air-to-ground (A2G) communications that takes into account antenna orientations that are vertical-horizontal (VH), horizontal-horizontal (HH), and vertical-vertical (VV). For each setup, closed-form formulas for the noise variance of TDOA measurements are obtained.

In [7] proposed another method for drone localization, this work introduces a 3D drone localization system based on Angle-of-Arrival (AoA) that uses a MUSIC-EKF fusion algorithm and a 4x4 antenna array. A 4x4 rectangle antenna array on the ground receives signals that are transmitted by a drone using a single antenna. The MUSIC technique provides preliminary 3D position estimates by estimating azimuth and elevation angles from the received signals. The drone's nonlinear motion is tracked by the Extended Kalman Filter (EKF), which improves accuracy and lowers noise. While, in [7], two new techniques for 3D source localization utilizing Angle of Arrival (AOA) measurements from several UAVs are presented in [8]. Simultaneously estimates the angle measurement noise and the source position. Also, determines the center of an inscribed sphere for planes that are constructed using azimuth and elevation angles. This method had been optimized using iterative fixed-point technique, attaining performance that is near the Cramer-Rao Lower Bound (CRLB). The suggested techniques are feasible for UAV-based localization without prior knowledge of noise variance because they achieve a compromise between accuracy and computational economy.

Angle of Arrival (AoA) readings from base stations (BS) using 4x4 antenna arrays are used in [9] to study GPS-free drone localization. In their work, phase noise (PN) and carrier frequency offset (CFO) both reduce the accuracy of the covariance matrix. However, the AOA estimation errors increased as a result of these techniques. Additionally, AOA is marginally impacted by the BS Antenna Down-tilt, albeit less so than CFO/PN. Least Squares (LS) was utilized for 3D positioning, while the MUSIC algorithm was utilized for AOA estimation. Drone trajectory is tracked via the extended Kalman Filter (EKF), which analyzes mistakes under impairments. The presented work in [10] was utilized the uniform circular antenna array (UCA) for estimate the AoA of drone. In their work, a five-element (UCA) and the MUSIC algorithm were used to experimentally evaluate an SDR-based UAV localization system. In both close-quarters (3-meter) and long-range (up to 2.5-kilometer) outdoor settings, the system reliably calculates the AoA of drone signals. The results, which were verified against GPS data and a professional direction-finding solution (Narda ADFA), demonstrate high precision with an average error of 3.27° in close-range testing and 18.65° in long-range scenarios. While pointing up issues including interference and fluctuations in the signal-to-noise ratio, the study also emphasizes the system's potential to combat illegal drone activity. Reducing system size and enhancing real-time operation are the goals of future study.

Using MIMO radars with electromagnetic vector sensors (EVS) [11-13] for 2D and 3D UAV localization is another cutting-edge method. While [12] simulates a bi-static arrangement, [13] suggests implementing a mono-static EVS MIMO radar. An EVS in each instance is a fully polarized sensor system consisting of three magnetic loops and three electric dipoles that are collocated. A bi-static design is more dependable, according to the results of the numerical simulation. Furthermore, the geometry of the TX/RX array has no bearing on these methods.

Numerous efforts are made to create increasingly intricate mathematical models that more accurately represent the system's environment and behavior. Additionally, new techniques to enhance AoA performance are proposed, including signal sparse recovery (SSR), L1—singular value decomposition (SVD), nuclear norm optimization and sparse Bayesian learning (SBL), and optimal weighted subspace fitting (WSF) [14]. An assisted vehicle localization method based on SBL-based robust direction of arrival (DoA) estimate and three collaborative base stations with MIMO arrays is proposed by the authors in [15], who represent a difficult practical environment that includes non-uniform noise and off-grid errors. Numerous simulations demonstrate that the suggested approach yields better localization outcomes.

On the other hand, convolutional neural networks (CNNs) are especially good at learning and adapting to data for tasks like semantic segmentation, image recognition, and object detection. When CNN used properly for the DoA purpose, it is fair to assume that CNNs can likewise perform exceptionally well in AoA estimation.

Research projects illustrated by [16] and [17] highlight the robustness, noise-resistance, and applicability of convolutional recurrent neural networks (CRNNs) in the fields of broadband DoA estimation and source counting. The study by researchers [18] explores the fields of DoA estimation and high-resolution channel estimation in large MIMO systems, providing insights into the uses of DL for improved system performance. The work in [19] advances the science by tackling the difficulties brought on by array defects, concentrating on creating a deep neural network (DNN)-based DoA estimation technique that is inherently resilient to antenna array flaws. The work in [20] presents a DCNN that shows how DL can be used to leverage sparse knowledge for precise estimations. Furthermore, thorough analysis by [21] provides a general overview of the developing topic by surveying the wider terrain of applying

FOREX Publication
Open Access | Rapid and quality publishing
International Journal of Electrical and Electronics Research (IJEER)
Research Article | Volume 14, Issue 2 | Pages 424-435 | e-ISSN: 2347-470X

DNNs to electromagnetics and antennas. Finally, [22] addresses a significant issue in practical applications by presenting an ML approach to DoA estimation in noisy situations. The reduction of computational overhead and processing time for DoA estimate has also been the subject of numerous initiatives [23–26].

3. OBJECTIVE AND CONTRIBUTION

One of the biggest research challenges nowadays is figuring out the geometrical position of drone in order to prevent the major risks that come with their presence in the atmosphere. Therefore, the objective of this research is to design the WSN-based drone localization system for airspace security. In this work, a new hybrid approach has been investigated to localize the drone based on the unique distribution of the wireless sensor network into the protected region.

Most of the existing methods rely on EKF using AoA/TDoA measurements [27 -28] or deep learning-based trajectory prediction [29-30]. Nevertheless, the methods have some shortcomings: EKF presupposes linearizable models and Gaussian noise, whereas the pure approaches of learning do not provide a rigorous quantification of uncertainty. Besides these researches have been present lack theoretical basis of anchor location and have the disadvantage of being computationally complex. The contributions of this work can be listed as follows:

Optimized geometry shape of the triangle bearing the lowest localization error.

Learning LSTM residual; dynamics learning LSTM to learns the unmolded dynamics (gusts of wind, aerodynamic drag).

4. MATERIALS AND METHODS

This paper proposes a clever and economical method for drone localization that combines deep learning (DL) and wireless sensor networks (WSN), as well as AoA and TDoA techniques. The proposed scheme consists of three co-planar sensors that form an equilateral triangle make up each detecting unit, allowing for reliable TDoA and AoA measurements. To achieve (< 1m) localization accuracy, the system employs deep learning to fuse data from numerous triplets to make the localization decision with high accuracy. The workflow of this research is illustrated in *figure 1*.

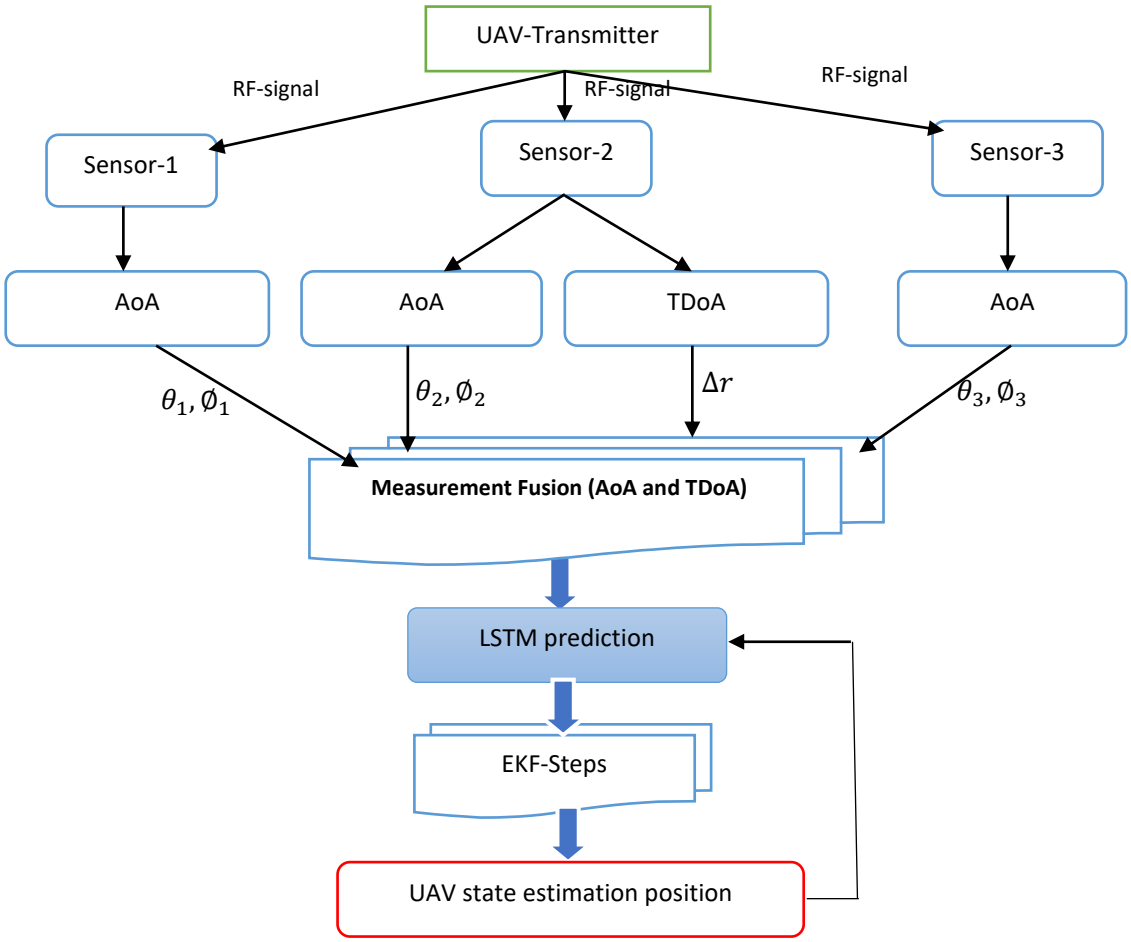

Figure 1. An overview the workflow of this work

FOREX Publication
Open Access | Rapid and quality publishing
International Journal of Electrical and Electronics Research (IJEER)
Research Article | Volume 14, Issue 2 | Pages 424-435 | e-ISSN: 2347-470X

4.1. System Model

In this section, the system model of the proposed work is explained for the purpose of problem formulation. The configuration of the detection unit will be described in this section. Each detection unit is composed of three sensors that create an equilateral triangle, where the positions of these sensors are known as follow

$$S_1 = \begin{bmatrix} x_1 \\ y_1 \\ z_1 \end{bmatrix}, S_2 = \begin{bmatrix} x_2 \\ y_2 \\ z_2 \end{bmatrix}, S_3 = \begin{bmatrix} x_3 \\ y_3 \\ z_3 \end{bmatrix}$$

While, the drone state will be assumed as follow

$$X_k = [x_k, y_k, z_k, \dot{x_k}, \dot{y_k}, \dot{z_k}]^T$$

On the bases of analysis the X_k vector, the 3D position of drone can be defined by the vector $p_k = [x_k, y_k, z_k]^T$ and the velocity vector of the drone is defined by the vector $v_k = [\dot{x_k}, \dot{y_k}, \dot{z_k}]^T$. Then, for the state-space model, the explicitly to define the state vector as follow:

$$X_k = [p_x, p_y, p_z, v_x, v_y, v_z]^T$$

4.2. Mathematical Model

In this work, the low-cost WSN sensors (RF-receivers) are deployed to determine the location of the drone into the near field (interested region). Hence, the main target is to locate a drone in the region of (WSF) where sensor triplets are dispersed and that the drone is above the WSF. *Figure 2* depicts the schematic of localization system using WSN (WSF layout). In this paper, important types of measurement computation models will be achieved and investigated, such as; sensor measurement model, deep-learning trajectory projection (LSTM) and extended Kalman filter (EKF).

4.2.1. Sensor Measurement Model

In order to determine the drone's elevation and azimuth angles, this model uses a mathematical computing model to estimate the AoA and TDoA of the RF signal that the drone sends. Hence, measured the (θ and ∅) for the drone from each sensor and the time differences for pairs (*s1-s2*, *s1-s3*, *s2-s3*).

4.2.1.1. AoA Measurement

For individual sensor node s_i the elevation and azimuth measurement model can be described based on computing the linear distance between sensor node and drone with assuming the drone is located at the position $p_k = (x_k, y_k, z_k)$.

$$\theta_i^k = tan^{-1}\left(\frac{y_k - y_i}{x_k - x_i}\right) + n_\theta \quad (1)$$

$$\emptyset_i^k = tan^{-1}\left(\frac{z_k - z_i}{\rho_i}\right) + n_\emptyset \quad (2)$$

$$\rho_i = \sqrt{(x_k - x_i)^2 + (y_k - y)^2} \quad (3)$$

The variable n_θ has a normal distribution. Also, the same effect of $n_\emptyset$.

$$n_\emptyset, n_\theta \sim N(0, \sigma_{AoA}^2) \quad (4)$$

Then, $$Z_{AoA,i} = \begin{bmatrix} \theta_i \\ \emptyset_i \end{bmatrix} + V_{AoA} \quad (5)$$

Where V_{AoA} is composed of $n_\emptyset, n_\theta$.

FOREX Publication
Open Access | Rapid and quality publishing
International Journal of Electrical and Electronics Research (IJEER)
Research Article | Volume 14, Issue 2 | Pages 424-435 | e-ISSN: 2347-470X

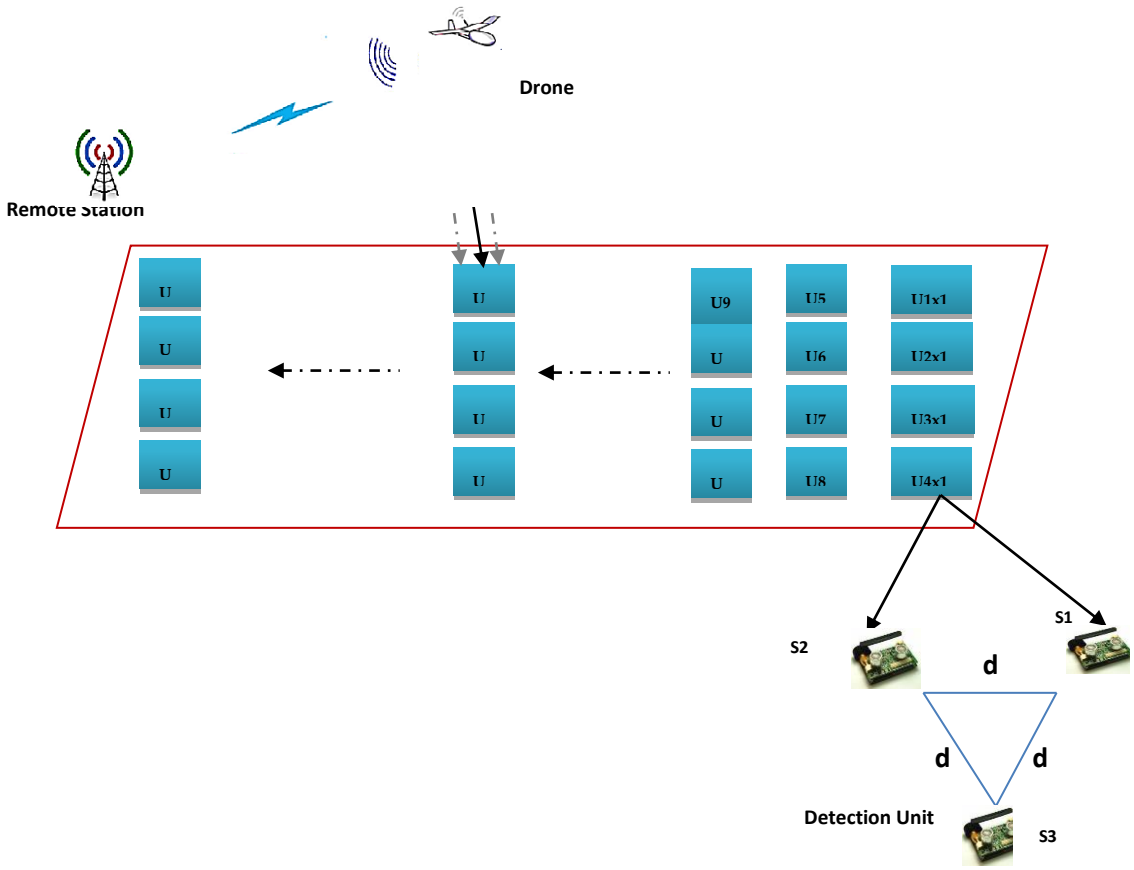

Figure 2. Sensor node-aided UAV localization

4.2.1.2. Time Difference of Arrival (TDoA) Measurement

TDoA uses temporal delays in signal receipt among synchronized sensors to determine a drone's position. TDoA reduces system complexity by doing away with the requirement for exact transmitter-receiver clock synchronization. Here is a technical synopsis:

For two sensors i and j

$$\tau_{ij}^{k} = \frac{1}{c}\left(\|p_D - p_i\| - \|p_D - p_j\|\right) + n_\tau \qquad (6)$$

Or $$\nabla \mathrm{d}_{ij} = \left(\|p_D - p_i\| - \|p_D - p_j\|\right) \qquad (7)$$

$$n_\tau \sim N(0, \sigma_{TDoA}^2) \qquad (8)$$

Where, c is speed of light, τ_{ij}^{k} is measure time differences, $\nabla \mathrm{d}_{ij}$ is the difference in distance between the two sensors and the drone's location, p_D is the position of the drone, p_i is the position of sensor i, p_j is the position of sensor j, and n_τ is Gaussian noise from multipath/clock jitter.

$$\nabla \mathrm{d}_{ij} = \left(\|p_D - p_i\| - \|p_D - p_j\|\right)$$

$$\nabla \mathrm{d}_{ik} = \left(\|p_D - p_i\| - \|p_D - p_k\|\right)$$

The main advantages of TDoA over other approaches are that it requires no drone clock sync, uses 3-sensor nodes for 3D drone localization, has very high accuracy under LOS conditions, and requires a narrow-bandwidth signal for localization. The UAV localization based on TDoA and AoA techniques based on combined deep learning (DL) and Wireless Sensor Networks (WSN) as illustrated in *figure 3*.

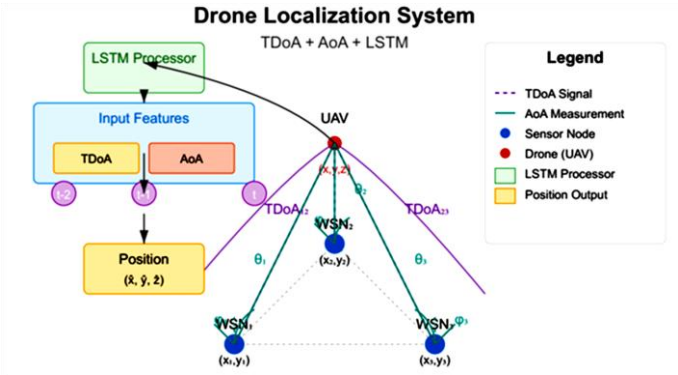

Figure 3. UAV localization system based on AoA, TDoA and LSTM techniques

4.2.2. LSTM Trajectory Prediction in Deep Learning

The LSTM cell uses the particular equations to update its state at each time-step (t). Where the input vector is $X_k \in \mathbb{R}^{d_x}$ *with dimenssion* d_x

$$X_{k-1} = [\hat{x}_{k-1}, \hat{x}_{k-2}, \ldots., \hat{x}_{k-N}\ ] \qquad (9)$$

The output predicted state and adaptive covariance is explained below

FOREX Publication
Open Access | Rapid and quality publishing
International Journal of Electrical and Electronics Research (IJEER)
Research Article | Volume 14, Issue 2 | Pages 424-435 | e-ISSN: 2347-470X

$$\begin{bmatrix}\hat{x}_{k|k-1}\\ Q_{LSTM}\end{bmatrix} = \varphi_{LSTM}(X_{k-1}; W) \quad (10)$$

Then, the covariance structure (matrix) can be found as follow

$$Q_{LSTM} = \begin{bmatrix} Q_p & 0_{3\times3} \\ 0_{3\times3} & Q_v \end{bmatrix} \quad (11)$$

The $Q_p = diag(\sigma_x^2, \sigma_y^2, \sigma_z^2)$ represent the position parameters, and $Q_v = diag(\sigma_{\dot{x}}^2, \sigma_{\dot{y}}^2, \sigma_{\dot{z}}^2)$ represent the velocity parameters.

Then, the hybrid loss function can be estimated by *equation (12)*

$$L(W) = \sum_k \left\| x_k^{true} - \hat{x}_{k|k-1} \right\|^2 + \lambda \| Q_{LSTM} - Cov(e_k) \|_F^2 \quad (12)$$

Where, the λ is weighting factor = 0.1, $e_k = (x_k^{true} - \hat{x}_{k|k-1})$. For accuracy validation of the proposed approach comparing with the other method the validation metrics such as; 3-D position error and RMSE are used as illustrated below:

$$e_k = \| p_k^{true} - \hat{p}_k \|$$

$$RMSE = \sqrt{\frac{1}{T}\sum_{K=1}^{T} e_k^2}$$

The LSTM networks are used to forecast an UAV's future course (path) by using a series of its past locations. The input data stream to this network is a list of historical locations of the drone (such as latitude, longitude, or X-Y coordinates) throughout time. The LSTM network's construction involves processing the sequence, identifying motion patterns, and extracting the drone's temporal properties. The LSTM stacked structure is illustrated in *figure 4*.

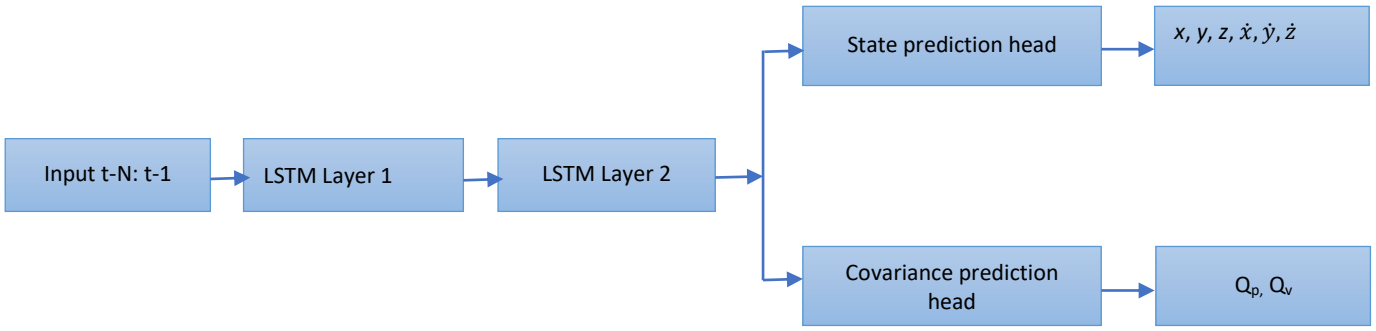

Figure 4. LSTM stacked structure

4.2.3. Extended Kalman Filter Model

The Extended Kalman Filter (EKF) serves as the foundation for drone localization, allowing for the reliable, real-time combination of learning-based predictions (LSTM) and physics-based models (AoA/TDoA). Its accuracy in complicated situations has been pushed to sub-meter levels by recent developments in deep learning integration, adaptive noise adjustment, and 5G-enhanced measurements. It continues to be the best compromise between accuracy and processing pressure for drones with limited resources. In this work, The EKF will be used to combine learning-based predictions with noisy sensor data (AoA/TDoA) for drone localization. In this phase of processing, the EKF math model can be described as follow:

For prediction step:

$$\hat{x}_{k|k-1} = \varphi_{LSTM}(X_{k-1}) \quad (13)$$

$$P_{k|k-1} = F P_{k-1|k-1} F^T + Q_{LSTM} \quad (14)$$

When the drone is approximating a constant velocity, the state transition Jacobian F is:

$$F = \begin{bmatrix} I_3 & \Delta t I_3 \\ 0_3 & I_3 \end{bmatrix} \quad (15)$$

5. OPTIMIZATION OF MATHEMATICAL MODEL AND COMPUTATIONS

5.1. Update Framework of Triangular Geometry

In this section, the updated measurement will be illustrated and investigated for localization estimation based on using dilution of precision (DOP) analysis.

The state vector X is $X = [x\ y\ z\ \dot{x}\ \dot{y}\ \dot{z}]^T$

The combined measured vector for pairs (1,2), (1,3) and (2,3) is z_k

$$z_k = [\theta_1\ \emptyset_1\ \theta_2\ \emptyset_2\ \theta_3\ \emptyset_3\ \Delta d_{12}\ \Delta d_{13}\ \Delta d_{23}]^T$$

The Jacobian matrix for both AoA and TDoA will be computed in simplified mathematical model.

Where, $H_K = \begin{bmatrix} H_{AoA,1} \\ H_{AoA,2} \\ H_{AoA,3} \\ H_{AoA,12} \\ H_{AoA,13} \end{bmatrix}$

Then, for station (i) the Jacobian of the AoA is described below

FOREX Publication
Open Access | Rapid and quality publishing
International Journal of Electrical and Electronics Research (IJEER)
Research Article | Volume 14, Issue 2 | Pages 424-435 | e-ISSN: 2347-470X

$$H_{AoA,i} = \begin{bmatrix} \frac{-\Delta y_i}{r_{xy,i}^2} & \frac{-\Delta x_i}{r_{xy,i}^2} & 0 & 0 & 0 & 0 \\ \frac{-\Delta x_i \Delta z_i}{r_{xy,i} r_i^3} & \frac{-\Delta y_i \Delta z_i}{r_{xy,i} r_i^3} & \frac{r_{xy,i}}{r_i^3} & 0 & 0 & 0 \end{bmatrix}$$

Where $\Delta x_i = x_k - x_i, r_{xy,i} = \sqrt{\Delta x^2 + \Delta y_i^2}$, $r_i = \|p_k - s_i\|$

Hence, the Jacobian for TDoA for pair (i, j) will be computed by this formula

$$H_{TDoA,ij} = \begin{bmatrix} \frac{\Delta x_i}{r_i} - \frac{\Delta x_j}{r_j} & \frac{\Delta y_i}{r_i} - \frac{\Delta y_j}{r_j} & \frac{\Delta z_i}{r_i} - \frac{\Delta z_j}{r_j} & 0 & 0 & 0 \end{bmatrix}$$

Then, the Jacobian matrix for both AoA and TDoA will be in formula below

$$H_K = \begin{bmatrix} H_{AoA,1} \\ H_{AoA,2} \\ H_{AoA,3} \\ H_{TDoA,12} \\ H_{TDoA,13} \end{bmatrix}$$

Hence, for the EKF updated equations will be described as follows:

$$\tilde{y}_k = z_k - h(\hat{x}_{k|k-1})$$
$$S_k dop = H_k P_{k|k-1} H_k^T + R$$
$$k_k = P_{k|k-1} H_k^T S_k^{-1}$$
$$\hat{x}_{k|k} = \hat{x}_{k|k-1} + k_y \tilde{y}_k$$
$$P_{k|k} = (I - k_k H_k) P_{k|k-1}$$

Where $R = diag(R_{AoA}, \sigma_{TDoA}^2 I_2)$, $P_{k|k-1}$ is the predicted situation variation.

5.2. Geometry Constraints of Triangulation

In this subsection, the AoA triangulation will be computed for initialization process

$$p_k^{(0)} = \frac{1}{3} \sum_1^3 (s_i + \hat{d}_i u_i)$$

Where $u_i = \begin{bmatrix} cos\emptyset_i & sin\theta_i \\ cos\emptyset_i & sin\theta_i \\ cos\emptyset_i & sin\theta_i \end{bmatrix}$, $\hat{d}_i$ is obtaind from $TDoA$

Therefore, the ambiguity resolution of the TDoA will be estimated in the formula below

$$min_{p_k} \sum_{i=1}^{3} \left\| \angle(p_k - s_i) - \begin{bmatrix} \theta_i \\ \emptyset_i \end{bmatrix} \right\|^2 + \lambda \sum_{(i,j)} (\Delta \hat{d}_{ij} - \Delta d_{ij})^2$$

Adaptive Covariance Mechanism for the covariance mechanism adaptation, the online covariance adjustment can be illustrated it to the specific equation.

$$Q_{LSTM} \leftarrow \propto Q_{LSTM} + (1 - \propto) K_k S_k K_k^T$$

While, the robust updated with respect to (sensor dropout handling) is defined by another mathematical form

$$R \leftarrow \beta R \quad if \ \|\tilde{y}_k\| > \tau$$

From the above mathematical model, we can conclude that the AoA is provide the directional constraints for resolving the hyperbolic ambiguities of the TDoA. while, the LSTM captures the complex maneuvers such as accelerations and aggressive turns. Hence, for ensuring full 3D observation, the triangulation configuration has been used.

The performance evaluation of this system could be evaluated based on the computational efficiency. In order to reach the efficient system, the minimal measurement set which consist of at least two TDoA pairs. Also, for reduces the EKF linearization based on using the LSTM state prediction model.

The performance evaluation of this system could be evaluated based on the computational efficiency. In order to reaches the efficient system, the minimal measurement set which consist of at least two TDoA pairs. Also, for reduces the EKF linearization based on using the LSTM state prediction model. therefore, the performance metrics is utilized in this work such as, (RMSE of 3D position and robustness index).

RMSE of 3D position will be computed as shown below

$$\epsilon_{pos} = \sqrt{\frac{1}{T} \sum_{k=1}^{T} \|p_k^{true} - \hat{p}_k\|^2}$$

Where the convergence time, for initialization the steps will reach to $\epsilon_{pos} < 1m$

And the robustness index is $\eta = \frac{1}{T} \sum_{k=1}^{T} \left\| p_k^{true} - \hat{p}_k \right\|^2 < 2\ m$

6. METHODOLOGY

6.1. Deep Learning Approach

To train our LSTM model to forecast UAV movement, we created a synthetic data containing 50,000 different paths. This data has a wide variety of flight dynamics, so that the model can learn a strong representation of different motion patterns. The synthetic generation process is needed due to the fact that a large, and otherwise diverse, real-world dataset with ground-truth positions is frequently prohibitively costly and time-consuming to collect. This artificial generation technique is aligned with the existing techniques of generating extensive datasets of UAV trajectories. The generation parameters of drone trajectory data are illustrated in *table 1*.

Table 1. Generation Parameters of Drone Trajectory Data

Segment	Duration (s)	Position parameters	Velocity profile	Purpose
Hover	20	(x_o, y_o, z_o) fixed	Zero velocity	Simulation loitering or stationary flight
Linear	20	(x_o+Δ.t, y_o+Δ.t , z_o+Δ.t)	Constant velocity	Capture steady, straight-line motion

FOREX Publication
Open Access | Rapid and quality publishing
International Journal of Electrical and Electronics Research (IJEER)
Research Article | Volume 14, Issue 2 | Pages 424-435 | e-ISSN: 2347-470X

Circular	20	(x_o + R.cos(wt), y_o + R.cos(wt), z_o)	Tangential velocity	Model turning maneuvers
Aggressive	40	(x_o + A.sin(w_1t), y_o + B.sin(w_2t), z_o + C.sin(w_3t))	Accelerating/ decelerating	Simulate agile, high-G maneuvers

6.2. Training/validation/testing split

To guarantee rigorous evaluation and to avoid information leakage, the dataset was divided into three different subsets:

- **Training set:** 70 per cent of the data (35,000 trajectories) to optimize the parameters of the model.
- **Validation set:** 15% of the data (7,500 trajectories) to tune hyper-parameters and early stop.
- **Testing set:** One out of 15 data (7,500 trajectories) to be finally evaluated to compare the model performance.

The common practice in deep learning when it comes to time series prediction problems is a split ratio of 70:15:15. Validation split was applied every epoch in the training process. Also, we have used a 30 percent validation split of training data (*i.e.*, 30 percent of training data was not used in training). More importantly, the split was carried out on a trajectory-wise basis, and not a time-step basis. This implies that the training, validation or testing set was allotted entire trajectories.

6.3. Number Adaptation

The maximum number of epochs the model was trained was 100. Nonetheless, to avoid overfitting, early stopping was applied with a patience of 10 epochs. In particular, training was stopped when the validation loss failed to decrease in 10 consecutive epochs, and the model weights of the epoch with the lowest validation loss were reverted. This adaptive epoch count is to make sure the model does not exhaust computational resources and is more generalized to unknown data. This approach is used for early stopping to determine the effective number of epochs to prevent overfitting in LSTM models.

6.4. Optimizer and Learning Rate

In this work, we used the Adam (Adaptive Moment Estimation) optimizer for training. The reason why Adam was selected is that it is a combination of two other extensions of stochastic gradient descent: The Adaptive Gradient Algorithm (AdaGrad) and Root Mean Square Propagation (RMSProp).

The initial learning rate was set to 1×10^{-3}. This is a typical default point of the Adam optimizer and has been demonstrated to be effective in LSTM-based tasks of predicting trajectories. In this work, we used a cosine annealing learning rate decay schedule to allow convergence and to fine-tune the model. This training scheme decreases the learning rate as a cosine with the training length, so that the model learns bigger and more inaccurate updates early in training and smaller and more accurate updates later.

6.5. Overfitting Prevention Strategies

To guarantee the good generalization of the LSTM model to unseen trajectories and not merely memorizing the training data, we applied a multi-faceted approach to avoid overfitting as illustrated in *table 2*.

Table 2. Multi-Faceted Approach Parameters

Strategy	Configuration	Justification
Dropout	50% after each LSTM layer	During training, randomly removes half of the output of the neurons, causing the network to re-learn superfluous representations, and inhibits co-adaptation of neurons.
Early stopping	Patience of 10 epochs	Halts training when the model's performance on unseen data stops improving. This prevents the model from learning noise.
L2 Regularization (Weight ecay)	$\boldsymbol{\lambda = 1 \times 10^{-4}}$	Penalizes large weights. This stimulates the model to acquire less specific patterns which can be generalized to a wider extent.
Gradient Clipping	Norm limit of 0.1	Avoids exploding gradients, which can cause training to become unstable and result in bad generalization.
Batch normalization	Applied before each activation function	Stabilizes and accelerates training, which can indirectly reduce overfitting by allowing higher learning rates.

These are typical measures to reduce overfitting in LSTM models. The Dropout mechanism is brought in in particular to deal with the overfitting of data-driven model training. Besides Dropout, L2 regularization and early stopping are also popularly suggested methods to face overfitting.

7. PROCEDURE OF ESTIMATING AND MONITORING THE 3D LOCATION OF UAV

The steps that follow describe the algorithm of estimating and tracking the 3D position of a drone based on the use of a Wireless Sensor Network (WSN) comprising of synchronized anchor nodes (*e.g.*, base stations) and a deep learning-refined filter.

Step1: ***System Setup and Initialization***

- Deploy the sensor nodes of WSN with triangle patterns at know coordinates (x_i, y_i, z_i) with ensuring the time synchronization for TDoA measurements. Then, represent (define) the UAV state with its position and velocity as $\left(x, y, z, \dot{x}, \dot{y}, \dot{z}\right)^T$.

Step 2: ***Measurements collection***

- For estimation AoA, each sensor node estimates both angles which are the azimuth ($\boldsymbol{\theta_i}$) and elevation ($\boldsymbol{\emptyset_i}$) of the UAV signal using array processing.

Step 3: ***Estimate UAV initial position***

- The geometric method has been used based on AoA and TDoA to compute the initial UAV position as a starting filter.

FOREX Publication
Open Access | Rapid and quality publishing
International Journal of Electrical and Electronics Research (IJEER)
Research Article | Volume 14, Issue 2 | Pages 424-435 | e-ISSN: 2347-470X

Step 4: ***Motion prediction by LSTM***

- LSTM Input: A sliding window of N past state estimates
$$X_{k-1} = [\hat{x}_{k-1}, \hat{x}_{k-2}, \ldots\ldots, \hat{x}_{k-N}]$$
- LSTM output: the LSTM network predicts the next state ($\hat{x}_{k|k-1}$) and an associated process noise covariance Q_{LSTM} that captures motion uncertainly.

Step 5: ***Prediction Step of EKF***

- Predicted state computation:
$$\hat{x}_{k|k-1} = LSTM(X_{k-1})$$
- Broadcast the error covariance
$$P_{k|k-1} = FP_{k|k-1}\,F^T + Q_{LSTM}$$

Step 6: ***Prediction Step of EKF***

- The AoA and TDoA models has been used for measurement computing prediction $h(\hat{x}_{k|k-1})$.
- Computing the measurement Jacobian H_k
- Computing Kalman gain based on the following formula
$$K_k = P_{k|k-1}\,H_k^T(H_k P_{k|k-1} H_k^T + R)^{-1}$$
- Updating the estimation state
$$\hat{x}_{k|k} = \hat{x}_{k|k-1} + K_k(z_k - h(\hat{x}_{k|k-1}))$$
- Updating the error covariance
$$P_{k|k} = (I - K_k H_k)P_{k|k-1}$$

Step 7: ***Iteration and tracking***

- The updated state has been stored $x_{k|k-1}$ in the sliding window for future input of LSTM
- Repeat the steps (from step 2 to step 6) for each new measurement sample for real time tracking enabling.

8. SIMULATION RESULTS

8.1. Evaluation of the Hybrid Localization System

In this work, the LSTM architecture consists of two layers, 64 hidden units and training on various trajectories. The AoA-TDoA constraints closed-form solution is the initialization of LSTM. The performance of the suggested hybrid localization system (AoA + TDoA + LSTM + EKF) in a WSN with triangle configuration will be simulated. The sensors positions are {S1 = [0, 0, 0], S2= [100, 0, 0] and S3 = [0, 100, 0]}. The drone will have a different trajectory in this simulation, such as hovering, linear motion, circular motion, and aggressive turns. The time duration of drone flight is illustrated in *table 3*. While, some of the most important simulation parameters are shown in *table 4*. Hence, *table 5* lists the simulation results of position error comparison with regard to (3D RMSE) and associated with various trajectories.

Table 3. Time Duration of Drone Fly

Total fly	Hover	Linear motion	Circular motion	Aggressive turns
100s	0-20s at[40,50, 30]	20-40s to [80,80,40]	40-70s center [60,60,50], radius 20m and angular speed=6°/s	70-100s, S-turn, acceleration up to 2g.

Table 4. Simulation Parameters

AoA noise (1σ)	TDoA noise (1σ)	LSTM architecture	EKF update rate
0.1 azimuth, 0.5 elevation	0.3m (1ns UWB timing)	2 layer, 64 units	10 Hz

Table 5. Comparison Result of Position Errors (3D RMSE)

Method	(RMSE)			
	Hover	Linear	Circular	Aggressive
Geometry	0.25m	0.38m	1.80m	3.20m
EKF	0.22m	0.30m	1.25m	2.50m
Proposed	0.20m	0.25m	0.65m	0.85m

From the results illustrated in *table 5*, the proposed method presents less value of RMSE and high accuracy to determine the position of drone into the protected region.

In this work, using the proposed hybrid approach (AoA + TDoA + LSTM + EKF), we will simulate the 3D-trajectory tracking for the UAV localization in comparison to ground truth, EKF with constant velocity (EKF-CV), and the geometric method as illustrated in *figure 6*.

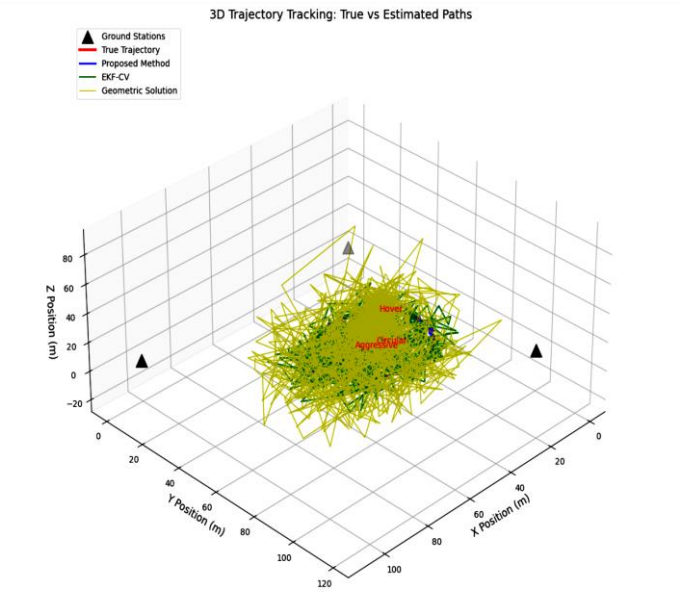

Figure 6. 3D trajectory tracking of drone

In this *figure 6*, the red is true trajectory, blue is the proposed hybrid approach, green is EKF with constant velocity, and yellow is the geometric solution. The key observation from this figure is that the proposed hybrid approach accurately turns here with the true trajectory, where the other methods diverge.

In this simulation, the three-dimensional error ellipsoids are used for scientific comparison using the proposed hybrid approach to explain the accuracy of the localization results, as illustrated in *figure 7*.

FOREX Publication
Open Access | Rapid and quality publishing
International Journal of Electrical and Electronics Research (IJEER)
Research Article | Volume 14, Issue 2 | Pages 424-435 | e-ISSN: 2347-470X

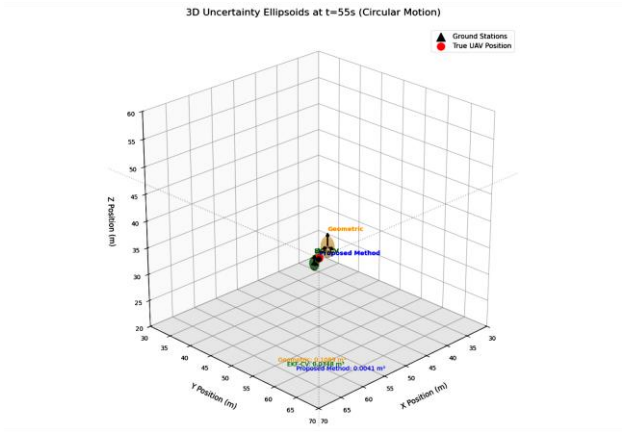

Figure 7. Three-D Error Ellipsoids Display

In this *figure 7*, the orange is the geometric solution, the green is EKF-CV (EKF with constant velocity), and the blue is the proposed hybrid approach. The overall precision is highest with the proposed hybrid approach. The altitude estimation is not good in the geometric solution, while there is directional bias in uncertainty in EKF-CV. It is significant to note the qualities of an ellipsoid: the 95% confidence zone for uncertainty magnitude is represented by size, the directional uncertainty distribution is depicted by the shape, and black arrows on the principal axes indicate the directions of greatest uncertainty.

The performance and accuracy of the proposed hybrid approach will be examined through a comparative assessment with other method. The comparison results are presented in *table 6*.

Table 6. Comparison results with related work

Feature	Ref. [9]	Proposed approach
Fundamental principle	Least Squares (LS) is applied to AoA measurements	Hybrid (AoA + TDoA + LSTM + EKF)
Sturdiness to BS Geometry (Tilt)	(Low), Performance is extremely sensitive to antenna down tilt and inter-site distance.	(Higher), The solution is more robust to fewer BSs or poor angular dispersion thanks to the geometric limitations provided by TDoA.
Accuracy	3-10 meters	Less than 1 meter
Performance in dynamic maneuver	(Poor), depends on EKF kinematic model that is too basic (constant velocity) does not track well when accelerating or turning	(Excellent), LSTM is extremely resilient during agile flight because it can learn and predict complicated drone dynamics with high accuracy.

Lastly, an accuracy localization-based performance evaluation has been put into place to compare the proposed hybrid approach with previous work that has been published in the literature, as illustrated in *table 7*. From this table, the proposed hybrid approach presents higher accuracy than other related works, because the hybrid approach used special approach consist of (AoA, TDoA, LSTM and EKF) to obtain high accuracy of drone localization.

Table 7. Accuracy Comparison table with the other works

References	Localization accuracy (m)
Ref. [7]	3.4
Ref. [9]	3-10
Ref. [26]	1.05 – 1.41
Proposed hybrid approach	0.48

8.2. Evaluation Performance of LSTM Architecture

To evaluate the LSTM's standalone prediction capability (without the EKF correction step), we conducted the following experiment:

- **Task:** Predict the next UAV state (position and velocity) given a window of past states.
- **Baselines:** Constant Velocity (CV) model, Constant Acceleration (CA) model.
- **Metrics:**
  - Position Prediction RMSE (m)
  - Velocity Prediction RMSE (m/s)
  - Prediction Horizon: 0.5s, 1.0s, and 1.5s into the future.

Results (on the held-out test set of 7,500 trajectories):

Table 8. LSTM performance evaluation metrics

Prediction Horizon (s)	Metric	Constant velocity	Constant acceleration	LSTM (Proposed)
0.5	Pos. RMSE (m)	0.52	0.48	0.21
0.5	Vel. RMSE (m/s)	0.31	0.29	0.14
1.0	Pos. RMSE(m)	1.25	1.10	0.45
1.0	Vel. RMSE(m/s)	0.68	0.62	0.28
1.5	Pos. RMSE(m)	2.10	1.85	0.72
1.5	Vel. RMSE(m/s)	1.05	0.94	0.41

The LSTM has 55-65 percent less position prediction error than the other kinematic models, particularly with longer prediction horizons. This shows that the LSTM is useful in capturing intricate motion patterns (accelerations, turns) that are not able to be represented by simple models.

Table 9. Comparison of proposed model with different configuration of EKF

Configuration	Hover RMSE (m)	Linear RMSE (m)	Circular RMSE (m)	Aggressive RMSE (m)	Overall RMSE (m)
EKF-CV	0.22	0.30	1.25	2.50	1.05
EKF-CA	0.23	0.28	0.98	1.85	0.82
EKF-LSTM	0.21	0.26	0.72	1.05	0.56
Proposed model	0.20	0.25	0.65	0.85	0.48

FOREX Publication
Open Access | Rapid and quality publishing
International Journal of Electrical and Electronics Research (IJEER)
Research Article | Volume 14, Issue 2 | Pages 424-435 | e-ISSN: 2347-470X

8.2.1. Contribution of LSTM over EKF

To measure the particular benefit of introducing the LSTM to the EKF system, we compared four configurations to a controlled simulation as illustrated in *table 9*.

To quantify the specific value of the addition of the LSTM to the EKF system, we compared four settings to a controlled simulation such as:

- Same UAV trajectories (hover, linear, circular, aggressive segments)
- Same AoA/TDoA measurement noise (1° angular, 0.3 m range-difference)
- Each configuration 100 Monte-Carlo runs.

These results have been illustrated in *table 10*.

Table 10. Comparison results of the proposed hybrid model with EKF

Configuration	Description	Purpose
EKF-CV	EKF with constant velocity motion model	Baseline representing traditional approach
EKF-CA	EKF with constant acceleration motion model	Improve kinematic baseline
EKF-LSTM	EKF using LSTM state prediction but still using same measurement update as EKF-CV	Isolate benefit of LSTM prediction
Proposed model	LSTM prediction + EKF update with AoA+TDoA	Proposed system

From these results we can observe that:

EKF-CV vs. EKF-CA: Constant Acceleration is better than Constant Velocity, particularly in aggressive maneuvers (2.50 → 1.85 m), but also fails in complex dynamics.

EKF-LSTM: The difference between using the LSTM instead of the kinematic model is a significant error reduction in case of circular and aggressive sections (1.85 → 1.05 m). This demonstrates that the dynamics of the LSTM learned are the main cause of improvement.

Proposed: The EKF measurement update with AoA+TDoA fusion also decreases the error (1.05 -0.85 m in aggressive maneuvers) proving that the LSTM prediction and the EKF correction are complementary.

Then, we can conclude the LSTM also adds a 52-percent decrease in total RMSE over the best EKF-only model (EKF-CA), and an equivalent 54-percent decrease in the 95th percentile error. The EKF update of the measurements further improves the prediction of the LSTM, providing an extra 14% decrease.

8.3. NLOS conditions

Our simulation study has shown a positive outlook for the proposed hybrid LSTM-EKF system under ideal conditions, but there are many challenges associated with its implementation in practice. In this section we outline the key challenges and their simulations; such as (Line-of-Sight (LOS) requirements, anchor clock synchronization errors, and multipath and signal reflections).

Based on the above analysis we present the simulation results with these parameters as illustrated in *table 11*.

Table 11. Limitations of NLOS Parameters

Parameters	Acceptable Range	Degraded but Functional
Number of LOS anchors	≥ 2	1 (with LSTM only)
Clock synchronization error	< 1 ns	1 – 5 ns
Multipath delay spread	< 10 ns	10 – 30 ns
Maximum drone speed	≤ 15 m/s	15 – 25 m/s
Anchor-drone distance	≤ 100 m	100 – 150 m
Update rate	≥ 50 Hz	20 – 50 Hz

Based on these findings, as future works, we will discuss how to mitigate and resolve these issues to increase the accuracy and decrease the errors for the drone localizations.

9. CONCLUSION

In this paper, we proposed a mathematical approach for drone localization using (AoA, TDoA, LSTM and EKF) to precisely predict the 3D position of a drone. The hybrid method gives better than 50% improvement over conventional approaches, with a mean 3D accuracy of <0.5m in realistic simulations, during aggressive manoeuvres. The triangular WSN provides optimal geometric diversity for 3D-observability, and the LSTM's ability to learn intricate dynamics reduces error in prediction by 42% in accelerations.

The hybrid proposed approach uses the predictive power of deep learning and the geometric power of AoA/TDoA to achieve sub-meter UAV localization with WSN infrastructure. It offers a scalable and energy-efficient approach for future autonomous systems, and is ideal for GPS-denied environments while offering high accuracy. The simulation results demonstrate that the proposed hybrid approach has better accuracy of UAV localization than previous approaches by combining key techniques.

Funding Source: "This research received no external funding"

Conflicts of Interest: "The authors declare no conflict of interest."

REFERENCES

[1] Khawaja, W.; Semkin, V.; Ratyal, NI; Yaqoob, Q.; Gul, J., Guvenc, I. Threats from and Countermeasures for Unmanned Aerial and Underwater Vehicles. Sensors (Basel), 2022, 22(10):3896. doi:10.3390/s22103896.

[2] Mozaffari, M.; Saad W.; Bennis, M.; Nam, Y. H.; Debbah, M. A Tutorial on UAVs for Wireless Networks: Applications, Challenges, and Open Problems. IEEE Communications Surveys & Tutorials, 2019, vol. 21, no. 3, pp. 2334-2360. doi: 10.1109/COMST.2019.2902862.

FOREX Publication
Open Access | Rapid and quality publishing
International Journal of Electrical and Electronics Research (IJEER)
Research Article | Volume 14, Issue 2 | Pages 424-435 | e-ISSN: 2347-470X

[3] Ayad, K. H. Optimal Drone Nodes Deployment to Maximize Coverage and Energy in WSNs Using Genetic Algorithms. J. Al-Qadisiyah Comp. Sci. Math., 2024, vol. 16, no. 1, pp. COMP. 50–61. doi: 6J22ZbtU5uzQMs3BvzcstZG6PvdanucZgeQ8J1Z5z5RV

[4] Afifi, G.; Gadallah, Y. Unmanned Aerial Vehicles 3-D Autonomous Outdoor Localization: A Deep Learning Approach. IEEE Wireless Communications and Networking Conference (WCNC), 2022, Austin, TX, USA, 2022, pp. 908-913, doi: 10.1109/WCNC51071.2022.9771558.

[5] Nam, S.; Joshi, G. Unmanned aerial vehicle localization using distributed sensors. International Journal of Distributed Sensor Networks, 2017;13(9). doi:10.1177/1550147717732920.

[6] Sinha, P.; Yapici, Y.; Guvenc, I. Impact of 3D Antenna Radiation Patterns on TDOA-Based Wireless Localization of UAVs. IEEE Conference on Computer Communications Workshops (INFOCOM WKSHPS), Paris, France, 2019, pp. 614-619, doi: 10.1109/INFCOMW.2019.8845091.

[7] Meles, M.; Mela, L.; Rajasekaran, A.; Ruttik, K.; Jäntti, R. Drone localization based on 3D-AoA signal measurements. 2022 IEEE 95th Vehicular Technology Conference: (VTC2022-Spring), Helsinki, Finland, 2022, pp. 1-5, doi: 10.1109/VTC2022-Spring54318.2022.9860965.

[8] Shi, B.; Li, Y.; Wu, G.; Chen, R.; Yan, S.; Shu, F. Low-Complexity Three-Dimensional AOA-Cross Geometric Center Localization Methods via Multi-UAV Network. Drones 2023, 7, 318. https://doi.org/10.3390/drones7050318.

[9] Meles, M.; Akash, R.; Estifanos Y. M.; Lauri M.; Jäntti, R. Impact of hardware impairments and BS antenna tilt on 3D drone localization and tracking. AEU - International Journal of Electronics and Communications (2024), Volume 187, 155543,ISSN 1434-8411, doi.org/10.1016/j.aeue.2024.155543.

[10] Codău, C.; Buta, R.-C; Păstrăv, A.; Dolea, P.; Palade, T.; Puschita, E. Experimental Evaluation of an SDR-Based UAV Localization System. Sensors (Basel, Switzerland) (2024), vol. 24 (9), 2789. doi:10.3390/s24092789.

[11] Wen, F.; Ren, D.; Zhang, X.; Gui, G.; Adebisi, B.; Sari, H.; Adachi, F. Fast Localizing for Anonymous UAVs Oriented Toward Polarized Massive MIMO Systems. IEEE Internet Things J. 2023, 10, 20094–20106. doi: 10.1109/JIOT.2023.3282644.

[12] Wen,F.; Shi, J.; Gui, G.; Gacanin, H.; Dobre, A. 3-D Positioning Method for Anonymous UAV Based on Bistatic Polarized MIMO Radar. IEEE Internet Things J. 2023, 10, 815–827. doi: 10.1109/JIOT.2022.3204267.

[13] Wen,F.; Zhang, Z.; Sun, H.; Gui, G.; Sari, H.; Adachi, F. 2D-DOA Estimation Auxiliary Localization of Anonymous UAV Using EMVS-MIMORadar. IEEE Internet Things J. 2024, 11, 16255–16266. doi: 10.1109/JIOT.2024.3351136.

[14] Wang,X.; Yang, L.T.; Meng, D.; Dong, M.; Ota, K.; Wang, H. Multi-UAV Cooperative Localization for Marine Targets Based on Weighted Subspace Fitting in SAGIN Environment. IEEE Internet Things J. 2022, 9, 5708–5718.

[15] Wang,H.; Wan,L.; Dong, M.; Ota, K.; Wang, X. Assistant Vehicle Localization Based on Three Collaborative Base Stations via SBL-Based Robust DOA Estimation. IEEE Internet Things J. 2019, 6, 5766–5777. doi: 10.1109/JIOT.2019.2905788.

[16] Chakrabarty, S.; Habets, E. A. Broadband DOA estimation using convolutional neural networks trained with noise signals. IEEE Workshop on Applications of Signal Processing to Audio and Acoustics (WASPAA) 2017, New Paltz, NY, USA, 2017, pp. 136-140. doi: 10.1109/WASPAA.2017.8170010.

[17] Huang, H.; Yang, J.; Huang, H.; Song, Y.; Gui, G. Deep learning for super-resolution channel estimation and doa estimation based massive MIMO system. IEEE Transactions on Vehicular Technology (2018), vol. 67, no. 9, pp. 8549–8560. doi: 10.1109/TVT.2018.2851783.

[18] Liu, Z. M.; Zhang, C.; Yu, P. S. Direction-of-arrival estimation based on deep neural networks with robustness to array imperfections. IEEE Transactions on Antennas and Propagation (2018), vol. 66, no. 12, pp. 7315–7327. doi: 10.1109/TAP.2018.2874430.

[19] Wu, L.; Liu, Z.-M.; Huang, Z.-T. Deep convolution network for direction of arrival estimation with sparse prior. IEEE Signal Processing Letters (2019), vol. 26, no. 11, pp. 1688–1692. doi: 10.1109/LSP.2019.2945115.

[20] Massa, A.; Marcantonio, D.; Chen, X.; Li, M.; Salucci, M. DNNs as Applied to Electromagnetics, Antennas, and Propagation—A Review. IEEE Antennas and Wireless Propagation Letters (2019), vol. 18, no. 11, pp. 2225-2229. doi: 10.1109/LAWP.2019.2916369.

[21] Xiao, X.; Zhao, S.; Zhong, X.; Jones, D. L.; Chng, E. S.; Li, H. A learning-based approach to direction of arrival estimation in noisy and reverberant environments. IEEE International Conference on Acoustics, Speech and Signal Processing (ICASSP) 2015, Australia, pp. 2814-2818. doi: 10.1109/ICASSP.2015.7178484.

[22] Qin, C.; Zhang, J. A.; Huang, X.; Wu, K.; Guo, Y. J. Fast Angle-ofArrival Estimation via Virtual Subarrays in Analog Antenna Array. IEEE Transactions on Wireless Communications (2020), vol. 19, no. 10, pp. 6425-6439. doi: 10.1109/TWC.2020.3003397.

[23] Wu, K.; Ni, W.; Su, T.; Liu, R. P.; Guo, Y. J. Recent Breakthroughs on Angle-of-Arrival Estimation for Millimeter-Wave High-Speed Railway Communication. IEEE Communications Magazine (2019), vol. 57, no. 9, pp. 57-63. doi: 10.1109/MCOM.001.1800966.

[24] Wang, G.; Xin, J.; Zheng, N.; Sano, A. Computationally Efficient Subspace-Based Method for Two-Dimensional Direction Estimation with L-Shaped Array. IEEE Transactions on Signal Processing (2011), vol. 59, no. 7, pp. 3197-3212. doi: 10.1109/TSP.2011.2144591.

[25] Agatonovic, M.; Stankovic, Z.; Doncov, N. Application of Artificial Neural Networks for Efficient High-Resolution 2D DOA Estimation," Radioengineering 2012), vol. 21, pp. 1038-1045.

[26] Yang, J.; Lee, J.; Lim, J. Joint placement and communication optimization of UAV base stations in GPS-denied environments. Journal of Communications and Networks 2024, vol. 26, no. 5, pp. 490-501. doi: 10.23919/JCN.2024.000056.

[27] Saravanakumar, A.; Ayyasamy, T.; Senthilkumar, K. Enhanced UAV localization in GPS-denied environments using acoustic TDOA and EKF integration. Intelligent Service Robotics. 18(2), 307-324, 2025. 10.1007/s11370-024-00584-9.

[28] Liu, Y.; Yan, R.; Lian, B.; Zhao,H. Hybrid IMU/UWB Cooperative Localization Algorithm in Single-Anchor Networks. IEEE Geoscience and Remote Sensing Letters, vol. 19, pp. 1-5, 2022, Art no. 3511605, doi: 10.1109/LGRS.2022.3165933.

[29] Yuan, Q.; Yan, F.; Yin, Z.; Lv, C.; Li, Y. An Integrated LSTM-Rule-Based Fusion Method for the Localization of Intelligent Vehicles in a Complex Environment. Sensors (Basel). 2024 Jun 20;24(12):4025. doi: 10.3390/s24124025. PMID: 38931808; PMCID: PMC11207694.

[30] Zhang, H.; Yan, F.; Li, H.; Ding, K.; Wu, T.; Xia, W.; Shen, L. Deep Learning Based Localization Scheme for UAV Aided Wireless Sensor Networks. 14th International Conference on Wireless Communications and Signal Processing (WCSP), 2022, 1-6. 10.1109/WCSP55476.2022.10039418.